Human Molecular Genetics, 2013, Vol. 22, No. 16 **3269–3282**
doi:10.1093/hmg/ddt182
Advance Access published on April 16, 2013

Glucocorticoid receptor is required for foetal heart maturation

Eva A. Rog-Zielinska[1], Adrian Thomson[1], Christopher J. Kenyon[1], David G. Brownstein[2], Carmel M. Moran[1], Dorota Szumska[4], Zoi Michailidou[1,3], Jennifer Richardson[1], Elizabeth Owen[1], Alistair Watt[3], Harris Morrison[6], Lesley M. Forrester[5], Shoumo Bhattacharya[4], Megan C. Holmes[1] and Karen E. Chapman[1,*]

[1]Centre for Cardiovascular Science, [2]Mouse Pathology Core and [3]MRC Centre for Inflammation Research, University of Edinburgh, Queen's Medical Research Institute, Edinburgh EH16 4TJ, UK [4]Wellcome Trust Centre for Human Genetics, Oxford OX3 7BN, UK [5]MRC Centre for Regenerative Medicine, University of Edinburgh, Edinburgh EH16 4UU, UK [6]MRC Institute of Genetics and Molecular Medicine, University of Edinburgh, Western General Hospital, Edinburgh EH4 2XU, UK

Received February 6, 2013; Revised March 27, 2013; Accepted April 12, 2013

Glucocorticoids are vital for the structural and functional maturation of foetal organs, yet excessive foetal exposure is detrimental to adult cardiovascular health. To elucidate the role of glucocorticoid signalling in late-gestation cardiovascular maturation, we have generated mice with conditional disruption of glucocorticoid receptor (GR) in cardiomyocytes and vascular smooth muscle cells using smooth muscle protein 22-driven Cre recombinase (SMGRKO mice) and compared them with mice with global deficiency in GR ($GR^{-/-}$). Echocardiography shows impaired heart function in both SMGRKO and $GR^{-/-}$ mice at embryonic day (E)17.5, associated with generalized oedema. Cardiac ultrastructure is markedly disrupted in both SMGRKO and $GR^{-/-}$ mice at E17.5, with short, disorganized myofibrils and cardiomyocytes that fail to align in the compact myocardium. Failure to induce critical genes involved in contractile function, calcium handling and energy metabolism underpins this common phenotype. However, although hearts of $GR^{-/-}$ mice are smaller, with 22% reduced ventricular volume at E17.5, SMGRKO hearts are normally sized. Moreover, while levels of mRNA encoding atrial natriuretic peptide are reduced in E17.5 $GR^{-/-}$ hearts, they are normal in foetal SMGRKO hearts. These data demonstrate that structural, functional and biochemical maturation of the foetal heart is dependent on glucocorticoid signalling within cardiomyocytes and vascular smooth muscle, though some aspects of heart maturation (size, ANP expression) are independent of GR at these key sites.

INTRODUCTION

Foetal glucocorticoid levels rise dramatically in late gestation in mammals, essential for maturation in preparation for life after birth (1). In mice, adrenal glucocorticoid synthesis, negligible at embryonic day (E) 14.5, increases rapidly from E15.5 to peak at E17.5 (2). Concurrently, maternal plasma glucocorticoid levels rise, peaking at E16–E17. Together with the late-gestation loss of the feto-placental 11β-hydroxysteroid dehydrogenase-2 (11β-HSD2) 'barrier' that inactivates maternal glucocorticoids (3), this dual-source surge in foetal glucocorticoid levels elicits structural, functional and biochemical changes in tissues and organs required for post-natal survival and adaption (1). Hence, synthetic glucocorticoids are routinely administered to mothers in preterm labour to accelerate foetal maturation, thus improving neonatal outcome (4), though premature activation of glucocorticoid-sensitive pathways may also have undesirable long-term side-effects (3).

Most glucocorticoid effects are mediated by the glucocorticoid receptor (GR), a member of the nuclear receptor superfamily of transcription factors. GR-deficient ($GR^{-/-}$) mice are glucocorticoid resistant and all born die soon after birth, principally due to lung immaturity (5), though effects on liver are also critical (6).

*To whom correspondence should be addressed. Tel: +44 1312426736; Fax: +44 1312426779; Email: karen.chapman@ed.ac.uk

When compared with most organs, the heart is functional relatively early in gestation and is required for foetal survival. In mice, the fundamental structural changes in heart development occur before E13.5. However, beyond E14.5, the heart continues to undergo extensive remodelling and maturation, reflected in changes in extracellular matrix composition, the expression of contractile proteins, metabolic maturation in preparation for higher postnatal energy demand and electrophysiological maturation of excitation–contraction systems. How these structural, functional, electrical and biochemical maturational changes are co-ordinated is largely unknown. Prenatally, glucocorticoids affect vascular responses (7,8). Direct effects on heart *in vivo* are unknown, although prenatal glucocorticoid treatment is reported to elicit growth-stimulatory (9,10) or inhibitory (11) effects on cardiomyocytes. Here, we show that mice globally lacking glucocorticoid signalling ($GR^{-/-}$ mice) have structurally and biochemically immature hearts with severely impaired function. To determine whether effects are direct within the cardiovascular system, we generated mice with conditional disruption of GR in cardiomyocytes and vascular smooth muscle cells (SMGRKO mice) using smooth muscle protein 22-driven Cre recombinase. The cardiomyocyte phenotype of SMGRKO mice closely resembles that of $GR^{-/-}$ mice, suggesting that GR in cardiomyocytes is essential to elicit critical maturational effects within foetal heart in late gestation. However, differences between the cardiac phenotype of SMGRKO and $GR^{-/-}$ mice suggest the phenotype is not entirely autonomous in cardiomyocytes and vascular smooth muscle.

RESULTS

Global abolition of glucocorticoid signalling severely impairs foetal heart function and causes *hydrops fetalis*

To address whether glucocorticoid signalling is required for foetal heart maturation, *Nr3c1*^{gtESK92MRCHGU} mice (12), heterozygous for a null allele of *Nr3c1* (the gene encoding GR), were intercrossed. Although $GR^{-/-}$ foetuses were present at the expected mendelian ratio at E14.5, prior to the surge in foetal glucocorticoid levels [37 (28%) $GR^{+/+}$, 62 (47%) $GR^{+/-}$ and 34 (26%) $GR^{-/-}$], they were present at half the number of $GR^{+/+}$ at E17.5 [140 (33%) $GR^{+/+}$, 217 (51%) $GR^{+/-}$, 68 (16%) $GR^{-/-}$; $P < 0.0001$, Pearson's χ^2 test], suggesting loss or death of some $GR^{-/-}$ foetuses between E14.5 and E17.5. Note that a previous study that reported normal viability of late gestation $GR^{-/-}$ foetuses (12) examined fewer foetuses (a total of 60) of which half were collected prior to E17.5. Histopathological examination of fixed sections of $GR^{-/-}$ foetuses showed they are grossly normal, but with immature lungs (consistent with previous findings) (5,13), kidneys (data not shown) and hearts.

Micro-magnetic resonance imaging and histopathological examination confirmed that heart size (measured as either total heart area or ventricular volume) is reduced in E17.5 $GR^{-/-}$ foetal hearts, despite correct development (Fig. 1). No differences are apparent in the configuration of the major vessels or the morphology of either the compact layer or trabeculae carnae (Fig. 1A and B). Reduced cardiomyocyte cell size in $GR^{-/-}$ hearts is indicated by more nuclei per field of view within comparable sections of the myocardium of $GR^{-/-}$ hearts ($GR^{-/-}$, 73 ± 4 nuclei per 10 000 μm^2 versus $GR^{+/+}$, 53 ± 2; $P < 0.001$, Student's *t*-test, $n = 5–7$).

Addressing function, *in vivo* ultrasound imaging of the left ventricle across the mitral valve of $GR^{-/-}$ foetuses shows a marked increase in the Doppler-derived myocardial performance index (MPI; a measure of combined systolic and diastolic function that is independent of heart rate and size) (14), indicating impaired heart function (Fig. 2A). Breakdown of the MPI into its three component parts shows increased contraction and relaxation times in $GR^{-/-}$ as well as $GR^{+/-}$ foetuses compared with wild-type littermates, though ejection times do not differ (Fig. 2B). The E/A wave velocity ratio (which normally increases in late gestation as diastolic function matures) (15) is lower in $GR^{-/-}$ foetuses compared with $GR^{+/+}$ (Fig. 2C). Early diastolic deceleration is decreased and early diastolic deceleration time/peak E wave velocity (mitral deceleration index) increased in $GR^{-/-}$ foetuses (Fig. 2D and E). Heart rate does not differ ($GR^{+/+}$ 244 ± 9, $GR^{+/-}$ 234 ± 4, $GR^{-/-}$ 250 ± 6, $P > 0.05$, ANOVA), nor does ejection fraction (Fig. 2F). These data unequivocally show impaired cardiac function, with diastolic function particularly affected, in late-gestation $GR^{-/-}$ foetuses (with heterozygotes intermediate).

Consistent with impaired heart function, though wet weight of E17.5 $GR^{-/-}$ foetuses (856 ± 19 mg) does not differ from $GR^{+/+}$ littermates (854 ± 36 mg), dry weight is reduced ($GR^{+/+}$ 118 ± 4 versus $GR^{-/-}$ 104 ± 2 mg; $P < 0.01$, Student's *t*-test, $n = 9–17$), suggesting fluid accumulation. This is supported by histology of fixed $GR^{-/-}$ foetuses which are visibly smaller than their $GR^{+/+}$ littermates (Supplementary Material, Fig. S1). Additionally, compared with $GR^{+/+}$, whole-body sodium levels are increased in E17.5 $GR^{-/-}$ carcasses ($GR^{+/+}$ 63.3 ± 1.3 versus $GR^{-/-}$ 70.9 ± 0.7 mmol/kg; $P < 0.01$, Student's *t*-test, $n = 9–17$) with no change in potassium ($GR^{+/+}$ 70.3 ± 1.3 versus $GR^{-/-}$ 69.0 ± 0.8 mmol/kg; $n = 9–17$), indicative of foetal oedema (*hydrops fetalis*) in E17.5 $GR^{-/-}$ mice. This phenotype could directly result from heart failure due to lack of glucocorticoid signalling within the heart and vasculature or could be indirect.

Deficiency in glucocorticoid signalling within cardiomyocytes and vascular smooth muscle impairs foetal heart function

To distinguish between the above possibilities, transgenic mice harbouring a Cre recombinase allele driven by the SM22 promoter (16) were used to generate SMGRKO mice, with disruption of the GR gene in cardiomyocytes and vascular smooth muscle. SM22-α protein is transiently expressed in the murine heart from E8.5 and in vascular smooth muscle from E9.5 (17) and SM22-Cre efficiently drives gene deletion in the foetal heart and vasculature (18,19). Levels of GR mRNA are reduced by 65% in E17.5 SMGRKO foetal hearts compared with controls ($GR^{fl/fl}$ Cre^{-}), with no difference in liver, lung or kidney (with adrenal) (Fig. 3A). Similarly, GR protein levels show a corresponding 65% reduction in E17.5 SMGRKO foetal hearts (Fig. 3B). Immunofluorescent and immunohistochemical labelling of GR showed that the residual GR in SMGRKO hearts is largely due to expression in cells other than cardiomyocytes and vascular smooth muscle (Fig. 3C and D). Consistent with normal GR expression outwith the

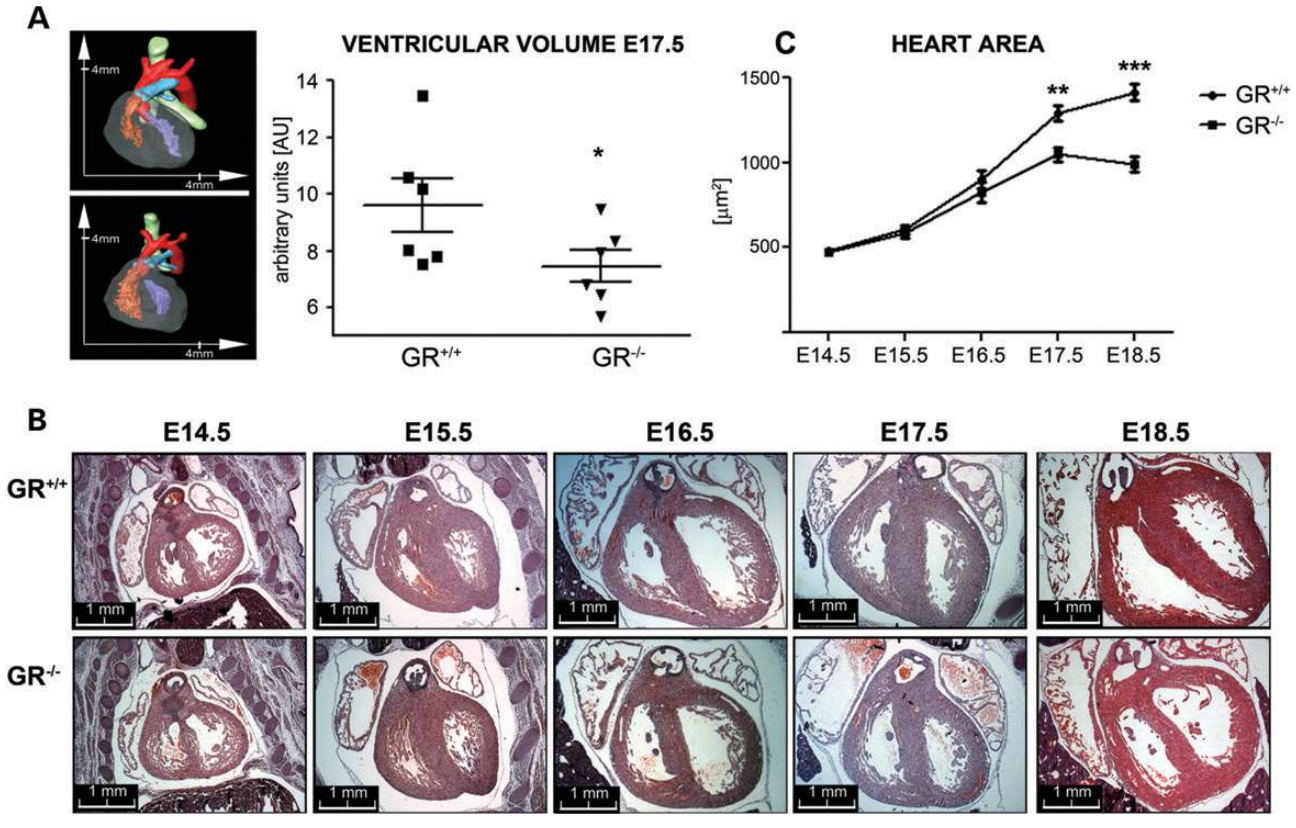

Figure 1. E17.5 $GR^{-/-}$ foetal hearts are correctly formed but smaller. (**A**) High-resolution magnetic resonance images show normal structure of E17.5 $GR^{-/-}$ foetal hearts (lower image) compared with $GR^{+/+}$ (upper image) and MRI measurements show reduced ventricular volume in E17.5 $GR^{-/-}$ foetal hearts (triangles) compared with $GR^{+/+}$ (squares). Data analysed by Mann–Whitney U-test. $^{*}P < 0.05$, $n = 6$. (**B** and **C**) Haematoxylin and eosin (H&E)-stained sections show $GR^{-/-}$ hearts (lower images) are smaller than $GR^{+/+}$ (upper images) at E17.5–18.5, with no structural abnormalities. Data analysed by two-way ANOVA with Bonferroni multiple comparisons *post-hoc* test ($n = 5$).

cardiovascular system, plasma corticosterone levels are normal in E17.5 SMGRKO mice (control $GR^{fl/fl}$ 575 ± 70 ng/ml versus SMGRKO 475 ± 52 ng/ml).

SMGRKO mice are present at the expected mendelian ratio at E17.5 [62 (55%) control $GR^{fl/fl}$, 51 (45%) SMGRKO] suggesting either that the loss of $GR^{-/-}$ foetuses may be independent of glucocorticoid signalling in the foetal cardiovascular system or that the residual 35% expression is sufficient for survival. However, cardiac function is impaired in SMGRKO foetuses, with an increase in the MPI resulting from increased isovolumetric contraction time (Fig. 3E). Isovolumetric relaxation time and E/A wave ratio are normal, suggesting normal diastolic function. Consistent with milder impairment of heart function, although oedema is still present, it is milder in SMGRKO foetuses with the percentage of body weight that is water, increased in SMGRKO mice compared with $GR^{fl/fl}$ controls (SMGRKO, wet weight 980 ± 20 mg; dry 229 ± 6 mg; 76.0 ± 0.5% body weight as water versus $GR^{fl/fl}$ controls, wet weight 939 ± 30 mg, dry 246 ± 8 mg; 73.5 ± 0.9% of body weight as water. $P < 0.05$, Student's *t*-test, $n = 17–24$). Additionally, compared with controls, whole-body sodium levels are increased in E17.5 SMGRKO carcasses (control $GR^{fl/fl}$ foetuses 64.0 ± 0.9 versus SMGRKO 67.0 ± 0.6 mmol/kg; $P < 0.05$, Student's *t*-test, $n = 17–24$) with no change in potassium (control $GR^{fl/fl}$ foetuses 62.8 ± 0.7 versus SMGRKO 63.1 ± 0.4 mmol/kg), consistent with oedema in E17.5 SMGRKO foetuses. Histopathological examination revealed no difference in foetal heart size between genotypes (control $GR^{fl/fl}$ foetuses 1374.3 ± 59.5 μm^2 versus SMGRKO 1377.0 ± 81.3 μm^2, Student's *t*-test, $n = 6–12$) but compared with controls, the number of nuclei per field of view is increased in comparable sections of the myocardium of E17.5 SMGRKO hearts (SMGRKO, 87 ± 4 nuclei per 10 000 μm^2 versus control $GR^{fl/fl}$, 76 ± 4; $P = 0.05$, Student's *t*-test, $n = 6–12$), suggesting smaller cell size.

Late-gestation $GR^{-/-}$ and SMGRKO hearts show similar cellular abnormalities including disorganized myofibrils and cellular alignment

As the compact myocardium matures, the muscle fibres in the outermost layer progressively change direction as the spiralling architecture develops. In wild-type hearts, the outer longitudinal muscle layer of the left ventricle is clearly delineated at E17.5, with rod-shaped cardiomyocytes aligned obliquely to the longitudinal axis of the heart (Fig. 4A). In contrast, myocardial cells in the outer layer of $GR^{-/-}$ hearts are irregularly shaped with little evidence of alignment (Fig. 4A). Like $GR^{-/-}$ foetal hearts, the outermost cells in the left-ventricular compact myocardium of E17.5 SMGRKO hearts fail to align and are irregularly shaped, in contrast to the clearly delineated layer of rod-shaped

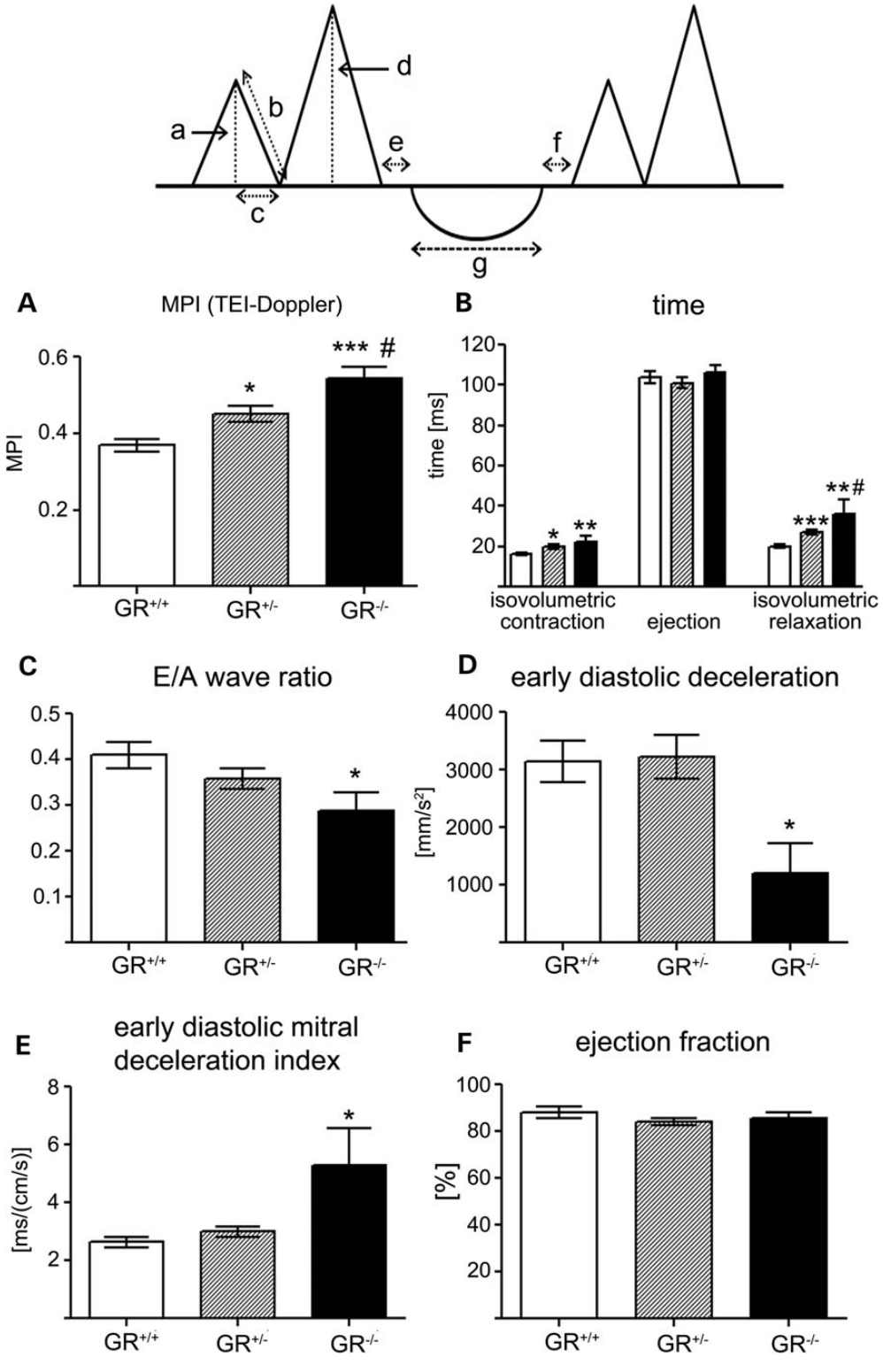

Figure 2. Severe impairment of cardiac function in E17.5 $GR^{-/-}$ foetuses. Top: Schematic representation of a typical mitral Doppler trace. Letters indicate: a, peak E wave velocity; b (slope of b), early diastolic deceleration; c, early diastolic deceleration time; d, peak A wave velocity; e, isovolumetric contraction time; f, isovolumetric relaxation time; g, ejection time. Specific parameters were calculated as follows: E/A wave ratio = a/d; MPI = (e+f)/g; early diastolic deceleration = b, early diastolic deceleration index = c/a. (**A–E**) *In vivo* Doppler velocity waveform measurements of left-ventricular function in E17.5 foetuses showing (A) increased myocardial performance (TEI-Doppler) index and (B) increased isovolumetric contraction and relaxation times in $GR^{-/-}$ and $GR^{+/-}$ foetuses compared with $GR^{+/+}$; (C) decreased E/A wave ratio in $GR^{-/-}$ compared with $GR^{+/+}$ littermates. (D) Early diastolic deceleration was lower and (E) deceleration time/peak E wave velocity (mitral deceleration index) higher in $GR^{-/-}$, indicative of diastolic dysfunction. There was no change in ejection fraction (**F**) between genotypes. $GR^{+/+}$, white bars; $GR^{+/-}$, hatched bars; $GR^{-/-}$, black bars. Data were analysed by two-way ANOVA with Bonferroni multiple comparisons *post-hoc* test. $^{*}P < 0.05$, $^{**}P < 0.01$ $^{***}P < 0.001$ versus $GR^{+/+}$; $\#P < 0.05$ versus $GR^{+/-}$, $n = 6–16$.

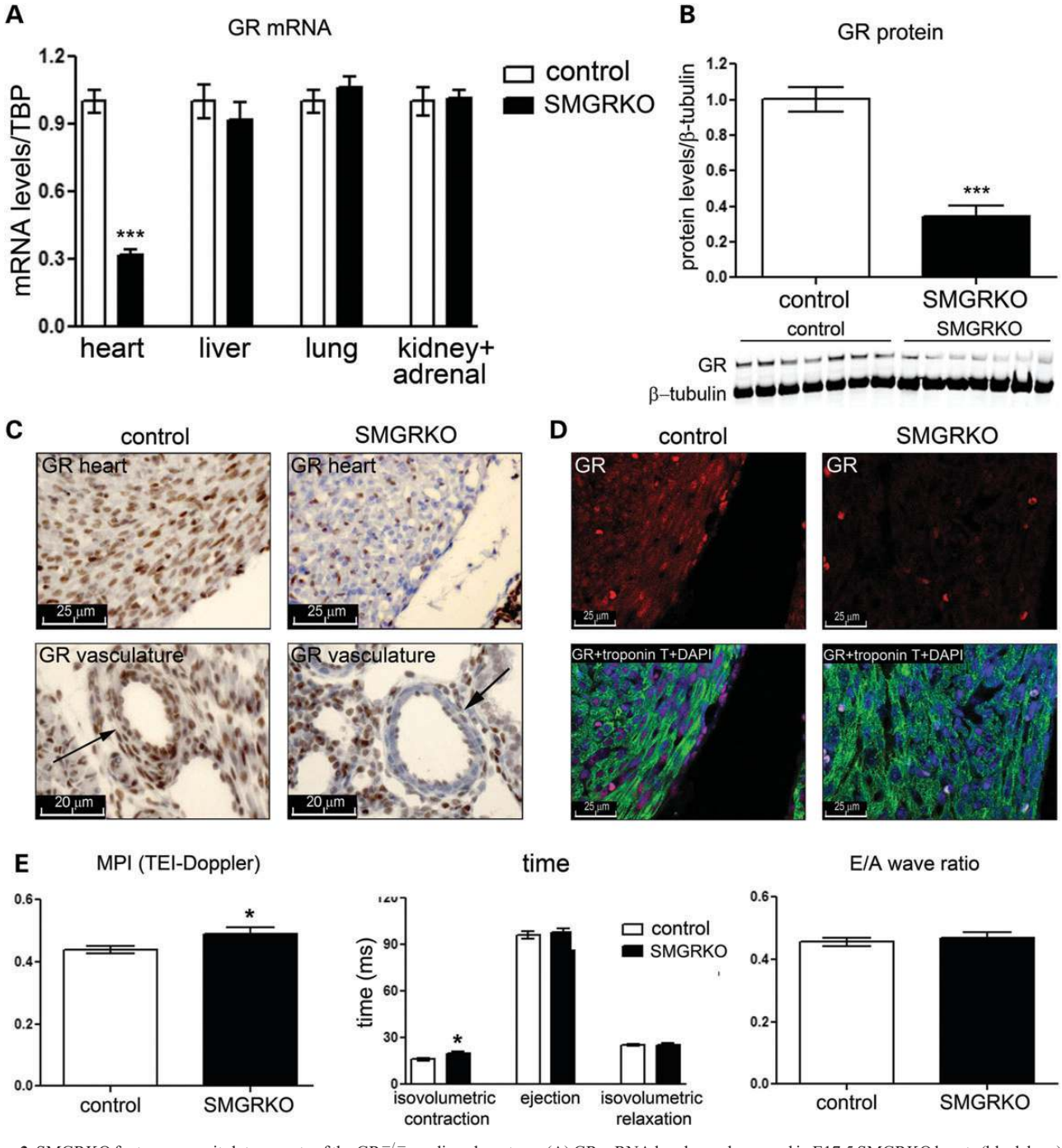

Figure 3. SMGRKO foetuses recapitulate aspects of the $GR^{-/-}$ cardiac phenotype. (**A**) GR mRNA levels are decreased in E17.5 SMGRKO hearts (black bars) compared with $GR^{fl/fl}$ controls (white bars), whereas levels in liver, lungs and kidney/adrenal are normal. (**B**) Levels of GR protein are similarly decreased in E17.5 SMGRKO hearts. For both (A and B), levels in the control group are arbitrarily set to 1. Data were analysed by Student's *t*-test, $^{***}P < 0.001$, $n = 7–10$. (**C**) The number of glucocorticoid receptor-expressing cells is reduced in SMGRKO myocardium and vascular smooth muscle layer. Representative ($n = 3$) images of GR-immunoreactivity in E17.5 ventricle and vasculature. GR (brown) is present in most nuclei (blue) within the heart and vascular smooth muscle cells (arrows) of control but not SMGRKO foetuses. (**D**) Glucocorticoid receptor is deleted from cardiomyocytes in SMGRKO foetuses. The number of GR (red)-immunoreactive cardiomyocytes (co-expressing troponin-T, green) is reduced in the ventricles of SMGRKO foetal hearts at E17.5. DAPI, nuclear counterstain. Arrows indicate non-cardiomyocyte cells expressing GR. (**E**) Increased myocardial performance (TEI-Doppler) index and increased isovolumetric contraction time in SMGRKO foetuses (black bars) compared with control ($GR^{fl/fl}$; white bars) indicate impaired left-ventricular function. E/A wave ratio is not different. Data were analysed by Student's *t*-test, $^{*}P < 0.05$, $n = 20–30$.

cardiomyocytes in control hearts (Fig. 4B). Transmission electron microscopy also shows similar phenotypes in $GR^{-/-}$ and SMGRKO hearts, with well-organized myofibrils in $GR^{+/+}$ and $GR^{fl/fl}$ control mice, but poorly aligned and disorganized myofibrils with only a few sarcomeres and less-defined Z-discs, in $GR^{-/-}$ and SMGRKO myocardium (Fig. 4C and D).

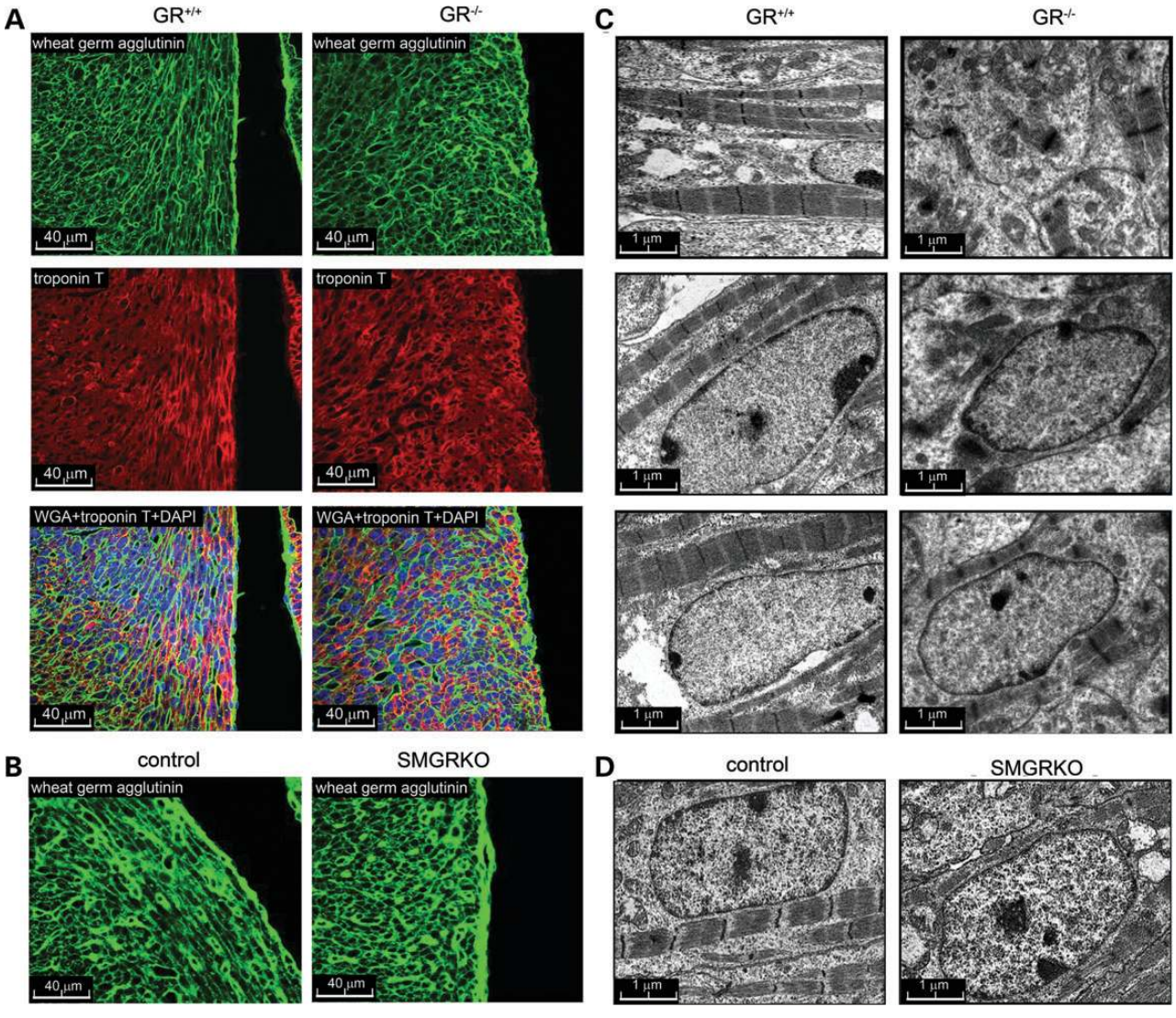

Figure 4. Late gestation $GR^{-/-}$ and SMGRKO hearts show abnormal cellular architecture. (**A** and **B**) Wheat germ agglutinin (WGA) plasma membrane staining shows abnormal cardiomyocyte shape and alignment in the left-ventricular myocardium of (A) E17.5 $GR^{-/-}$ hearts (right) compared with $GR^{+/+}$ (left) and (B) E17.5 SMGRKO hearts (right) compared with $GR^{fl/fl}$ controls (left). Images representative of $n = 4$. For (A), upper panels, WGA, middle panels, troponin T, lower panels, merged, with DAPI to stain nuclei. (**C** and **D**) Transmission electron micrographs of (C) E17.5 $GR^{+/+}$ (left panels) and $GR^{-/-}$ hearts (right panels) and (D) E17.5 $GR^{fl/fl}$ control (left panels) and SMGRKO hearts (right panels) showing immature, disorganized myofibrils in $GR^{-/-}$ and SMGRKO hearts. Images representative of $n = 5$.

RNA analysis suggests late-gestation $GR^{-/-}$ hearts are functionally immature

To explore mechanism, mRNAs encoding proteins relevant to cardiac function and maturity were measured. Levels of mRNA encoding MyHCα (the major contractile protein in adult hearts) increase in $GR^{+/+}$ between E14.5 and E17.5. However, while $GR^{-/-}$ hearts show normal MyHCα expression at E14.5, they lack the maturational increase at E17.5 (Fig. 5). MyHCα protein levels are similarly decreased in E17.5 $GR^{-/-}$ hearts compared with $GR^{+/+}$ (Fig. 6). The same is true of genes encoding calcium-handling proteins (NCX1, SERCA2a, RyR2; the sodium–calcium exchanger, the cardiac sarcoplasmic reticulum calcium ATPase and the cardiac ryanodine receptor, respectively) (Fig. 5), suggesting immature excitation–contraction coupling and calcium-induced calcium release in $GR^{-/-}$ foetal hearts. Together with reduced MyHCα, this provides a plausible mechanistic explanation for the impaired contraction/relaxation of late-gestation $GR^{-/-}$ hearts. Similarly, $GR^{-/-}$ hearts fail to induce expression of genes involved in energy metabolism that underpin late-gestation cardiac maturation (PGC1α, PFKFB2; peroxisome proliferator-activated receptor gamma coactivator 1-α, 6--phosphofructo-2-kinase/fructose-2,6-biphosphatase 2, respectively, and hexokinase-1) (Fig. 5). Immaturity in E17.5 $GR^{-/-}$ foetal hearts is further supported by lack of the normal maturational increase in mRNA encoding atrial natriuretic peptide (ANP), but importantly, expression of mRNA encoding the morphogenetic transcription factors GATA-4 and BMP-10 and the developmental regulator KLF-2 is normal in $GR^{-/-}$ foetal hearts (Fig. 5), consistent with correct development. GILZ

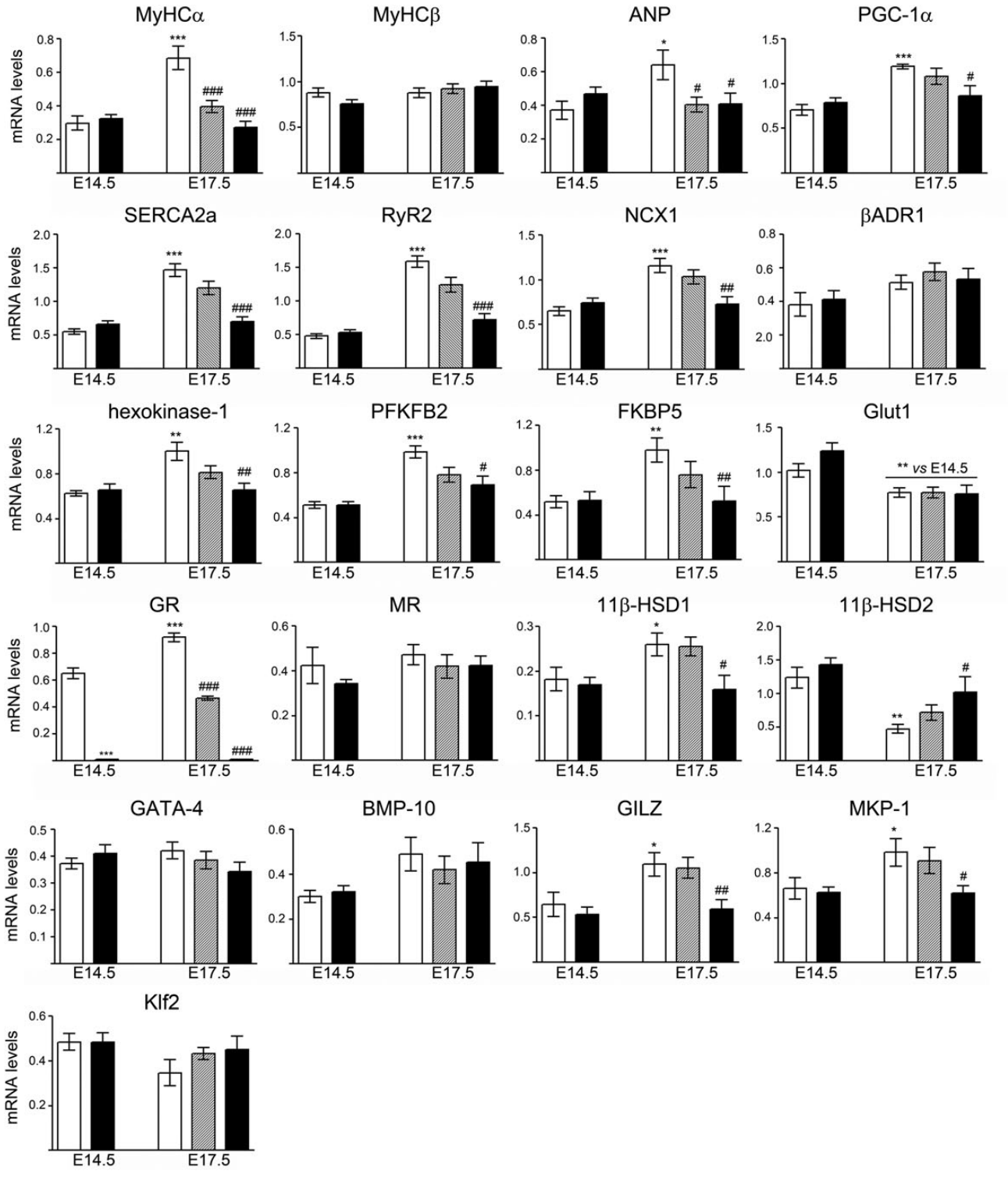

Figure 5. E17.5 $GR^{-/-}$ hearts show an immature transcriptome. qPCR measurement of specific mRNAs in E14.5 and E17.5 $GR^{+/+}$ (white), $GR^{+/-}$ (hatched) and $GR^{-/-}$ (black) foetal hearts. Data analysed by two-way ANOVA with Bonferroni multiple comparisons *post-hoc* test. $^{*}P < 0.05$, $^{**}P < 0.01$, $^{***}P < 0.001$ versus E14.5 $GR^{+/+}$; $\#P < 0.05$, $\#\#P < 0.01$, $\#\#\#P < 0.001$ versus E17.5 $GR^{+/+}$, $n = 7–13$.

(glucocorticoid-induced leucine zipper protein), classically glucocorticoid-regulated (20) is induced between E14.5 and E17.5 in $GR^{+/+}$ foetal hearts but not in $GR^{-/-}$. Other glucocorticoid-regulated genes (encoding MKP-1, FKBP5; respectively MAP kinase phosphatase-1 and FK506-binding protein-5) and the glucocorticoid metabolising enzymes, 11β-HSD1 and 11β-HSD2 (themselves glucocorticoid-regulated) (21,22) show similar lack of regulation between

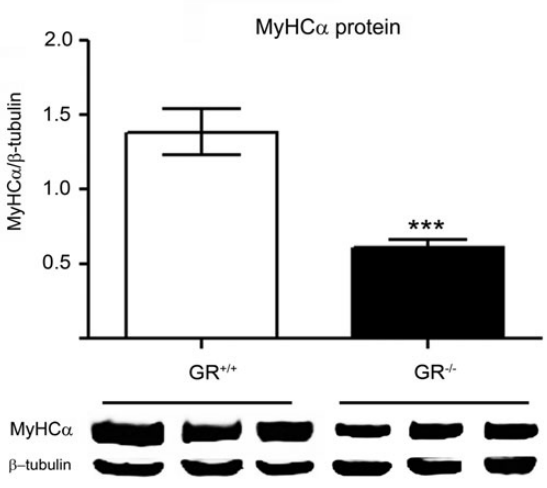

Figure 6. Reduced MyHCα protein levels in E17.5 $GR^{-/-}$ foetal hearts. Representative image and quantification of western blot showed MyHCα protein levels are decreased in E17.5 $GR^{-/-}$ hearts. Data were analysed by *t*-test. $^{***}P < 0.001$, $n = 6$.

E14.5 and E17.5 in $GR^{-/-}$ foetal hearts (Fig. 5). Of note, there are no compensatory changes in mRNA encoding mineralocorticoid receptor (MR) in $GR^{-/-}$ hearts (Fig. 5), nor are there any maturational changes in MR mRNA levels in wild-type mice.

Quantification of mRNA levels in E17.5 SMGRKO hearts shows qualitatively similar results to $GR^{-/-}$ foetal hearts for most mRNAs examined, though generally speaking, the magnitude of the effect is reduced (to a similar or slightly greater extent to $GR^{+/-}$ foetuses), suggesting the possibility of a gene-dosage effect of GR. Thus, levels of mRNA encoding the crucial calcium-handling proteins, SERCA2a and RyR2 are reduced in SMGRKO hearts at E17.5, as are levels of mRNA encoding hexokinase-1 and FKBP5 (Fig. 7), the latter a primary glucocorticoid target (20), consistent with diminished glucocorticoid signalling in SMGRKO hearts. However, there are important differences to $GR^{-/-}$ foetal hearts. Whereas levels of ANP are reduced in both E17.5 $GR^{-/-}$ and $GR^{+/-}$ hearts (the latter with 50% reduction in GR expression in heart; Fig 5), levels in E17.5 SMGRKO hearts are normal, suggesting that the reduction in ANP mRNA levels in $GR^{-/-}$ hearts occurs independently of glucocorticoid signalling in foetal cardiomyocytes and vascular smooth muscle. Similarly, levels of mRNA encoding MHCα are not significantly reduced in E17.5 SMGRKO hearts (Fig. 7) despite a significant reduction in $GR^{+/-}$ as well as $GR^{-/-}$ foetal hearts (Fig. 5).

GR is expressed in foetal heart from mid-gestation, but glucocorticoid levels in heart are negligible before late gestation

The similarities in heart phenotype between late-gestation $GR^{-/-}$ and SMGRKO foetuses suggest direct glucocorticoid signalling in cardiomyocytes. To address the presence and timing of receptor expression and ligand availability in heart, both were examined. *Nr3c1*^{gtESK92MRCHGU} mice contain a β-*geo* cassette (encoding β-galactosidase) at the GR gene locus, allowing for visualization of GR expression by X-gal staining. No staining is observed in E9.0 embryos (data not shown). X-gal staining is apparent at E10.5, restricted to the embryonic heart and the third brachial pouch (Fig. 8A). At E11.5, optical projection tomography (OPT) microscopy showed most of the X-gal staining to be in the myocardium and the major blood vessels of the whole embryo (Supplementary Material, Video). At E14.5 and later time points, staining appears throughout the myocardium and is widespread in other tissues (Fig. 8A and data not shown). Corticosterone levels in the heart are below the limit of detection at E14.5 and earlier times but rise dramatically at E15.5, peaking at E16.5 (Fig. 8B). Consistent with this, GR-immunoreactivity is present in troponin T^+ cardiomyocytes by E10.5 but is restricted to the cytoplasm prior to E14.5 (Fig. 8C). However, at E15.5 and E16.5, GR staining becomes intense in nuclei (Fig. 8C). Thus, widespread activation of GR driven by ligand availability in cardiomyocytes, commences at E15.5, further supporting the hypothesis that the cardiac phenotype of $GR^{-/-}$ foetuses results from lack of glucocorticoid signalling within the heart and vasculature.

DISCUSSION

Qualitatively, key aspects of the cardiac phenotype of SMGRKO foetal mice resemble that of $GR^{-/-}$ mice, demonstrating dependence of late-gestation foetal heart maturation upon glucocorticoid signalling in cardiomyocytes and vascular smooth muscle. Importantly, other aspects of the phenotype are distinct (summarized in Table 1).

Impairment of cardiac function is seen in both $GR^{-/-}$ and SMGRKO foetuses at E17.5, with increased MPI and prolonged isovolumetric contraction time, probably underpinned by the disorganized myofibrillar structure and lower expression of RyR2 seen in both $GR^{-/-}$ and SMGRKO foetal hearts. Interestingly, although SERCA2a expression is also significantly affected in both $GR^{-/-}$ and SMGRKO, relaxation is unaltered in SMGRKO mice, suggesting that under these circumstances, SERCA2A mRNA levels are not rate-limiting in foetal heart relaxation. The lower E/A wave ratio (diastolic function) in $GR^{-/-}$ foetuses suggests low compliance and/or increased stiffness due to deficient relaxation and/or recoil of the ventricular muscle (15) and is consistent with the longer relaxation time in these mice. In contrast, E/A wave ratio is normal in SMGRKO mice.

Structural immaturity is likely to underlie the functional immaturity. Remarkably, the structural and ultrastructural abnormalities of $GR^{-/-}$ mice are reproduced in SMGRKO mice. In both models, GR deficiency results in the failure of cardiomyocytes to align within the compact myocardium, possibly reflecting an inability to develop the normal spiralling architecture of the compact myocardium that is associated with maturing systolic and diastolic function (23). Increased myofibril content of myocardial fibres underpins the normal maturational changes in cardiac function (15) but myofibrils are short and disorganized in both $GR^{-/-}$ and SMGRKO foetal hearts. Plausibly, reduced levels of MyHCα in $GR^{-/-}$ foetal hearts could contribute to the impaired ultrastructure and function at E17.5; adult mice with ∼70% normal MyHCα levels show impaired cardiac contraction and relaxation (24). Moreover, the inferred decrease in MyHCα/β ratio in $GR^{-/-}$ foetal hearts (MyHCβ mRNA

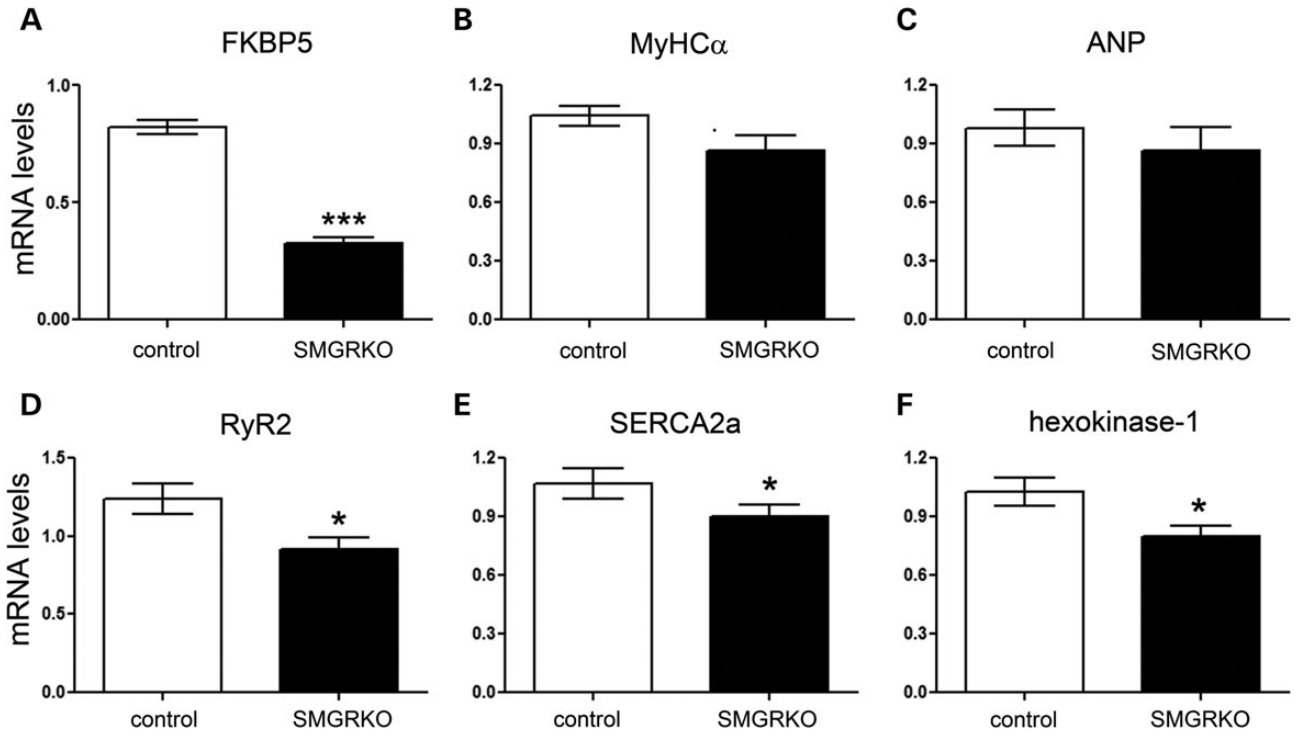

Figure 7. E17.5 SMGRKO hearts replicate some of the gene expression changes of E17.5 $GR^{-/-}$ foetal hearts but not others. qPCR measurement of specific mRNAs in E17.5 control (white) and SMGRKO (black) foetal hearts. Data analysed by Student's *t*-test $^{*}P < 0.05$, $n = 10$.

levels were unchanged) is consistent with decreased cardiac function as MyHCα/β ratio correlates directly with overall cardiac performance in adult animals (25) and in patients with cardiomyopathy and heart failure (26). However, the reduction in MyHCα mRNA levels in SMGRKO hearts was not statistically significant although $GR^{+/-}$ mice (with 50% reduction in GR) show a significant reduction in cardiac MyHCα equal to that seen in $GR^{-/-}$ foetuses. Therefore the alterations in MyHCα expression are unlikely to account for the ultrastructural differences conserved between SMGRKO and $GR^{-/-}$. Perhaps extrinsic actions of glucocorticoid signalling, for example via other hormonal systems (such as thyroid hormone signalling), are important in the aspects of cardiomyocyte maturation, including the increase in cardiac MyHCα content in late gestation.

The excess fluid that accumulates in $GR^{-/-}$ foetuses is of extracellular origin (indicated by the imbalance in sodium and sodium/potassium ratio) highlighting an important role for glucocorticoids in regulating fluid movement between the vascular and interstitial spaces. This must reflect, at least in large part, GR actions in cardiomyocytes and/or vascular smooth muscle, as SMGRKO foetuses also show foetal oedema, although to a lesser extent. Clinically, cardiogenic *hydrops* presents with inadequate diastolic ventricular filling (27), as seen in $GR^{-/-}$ foetuses, though not in SMGRKO. Impaired contractility of $GR^{-/-}$ and SMGRKO hearts might contribute to congestive heart failure. Although detailed histopathological analysis did not reveal any obvious abnormalities in the vessel structure of E17.5 $GR^{-/-}$ foetuses (unpublished data), vascular integrity could be compromised with GR-deficiency, leading to oedema. However, the more severe oedema in $GR^{-/-}$ foetuses suggests a greater involvement than just cardiomyocytes and vascular smooth muscle and might reflect placental and/or renal actions of GR. Whether the electrolyte imbalance is partly a reflection of the latter is currently unclear. GR-mediated glucocorticoid effects on renal electrolyte homeostasis have been reported (28–30). Moreover, proximal tubule development is severely impaired in E17.5 $GR^{-/-}$ foetuses (unpublished data), and the resulting renal deficit could plausibly affect fluid homeostasis, despite the limited reliance on the foetal kidney for blood filtration.

In the foetus, cardiac ANP responds to volume stimuli and regulates blood pressure and salt/water balance. Reduced levels of cardiac ANP mRNA in foetal $GR^{-/-}$, but not SMGRKO, suggest that volume and blood pressure regulation in foetal SMGRKO mice is normal. Indeed, whereas $GR^{+/-}$ mice are hypertensive (12), blood pressure is normal in adult SMGRKO mice, which survive to adulthood (though females are underrepresented at weaning) and which have a grossly normal phenotype in terms of appearance, body weight and behaviour, though cardiac hypertrophy is apparent at 12 weeks of age (R.V. Richardson, E. R.-Z., K.E.C., unpublished data). The detailed cardiac phenotype of adult SMGRKO mice will be published separately. Importantly, normal cardiac ANP levels also suggest normal placental vascular supply (31) in SMGRKO, but perhaps not in $GR^{-/-}$ foetuses with their reduced cardiac ANP expression. Lack of ANP reduces foetal survival (32) suggesting that the reduced survival of $GR^{-/-}$ foetal mice may be attributable to reduced ANP, with normal levels of ANP and normal survival observed in SMGRKO foetal mice. Thus, this aspect of the phenotype appears independent of GR in cardiomyocytes and vascular smooth muscle. The locus of the effect will be important to determine, but candidates include a role

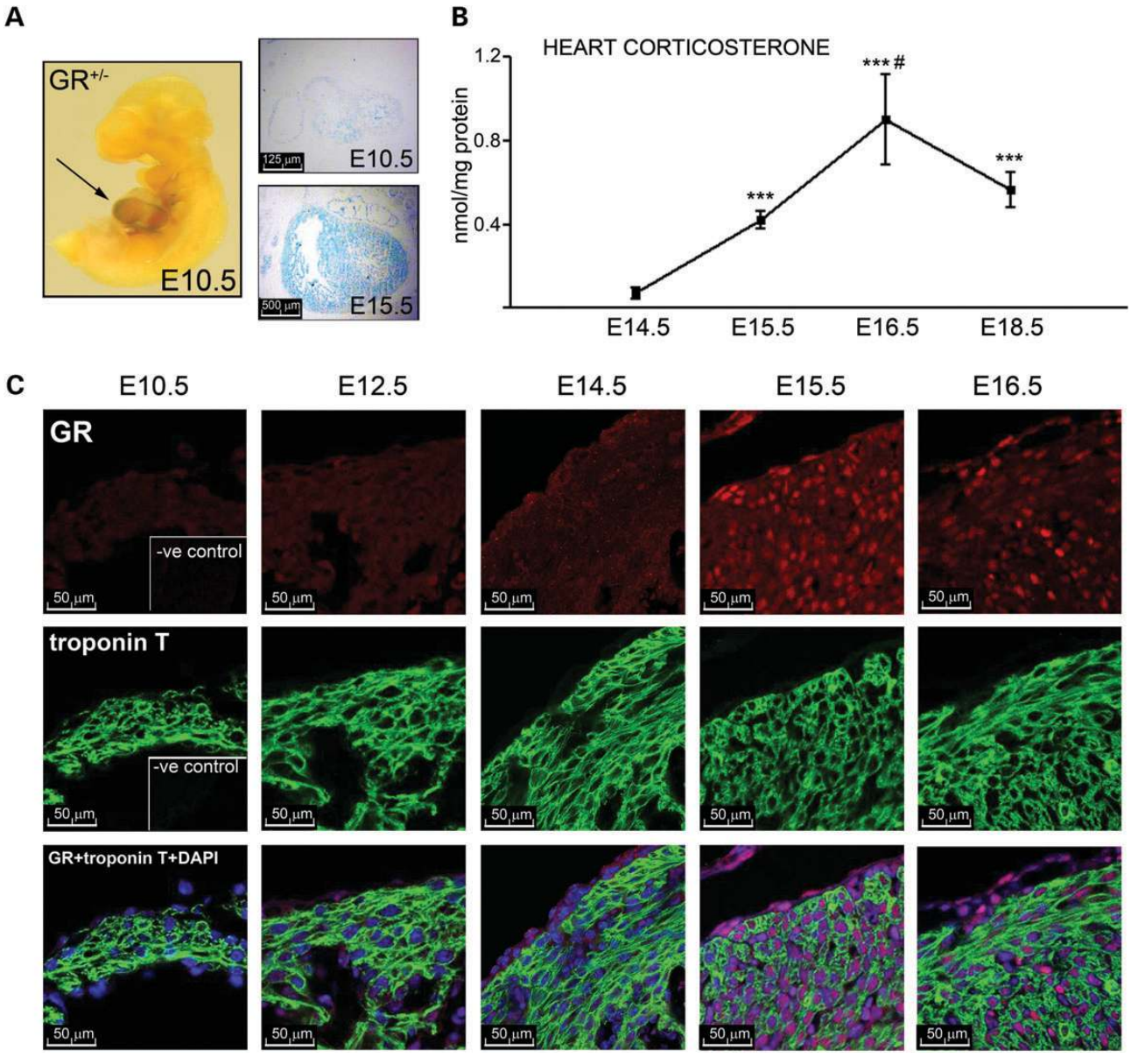

Figure 8. GR is expressed in the foetal heart from E10.5 yet corticosterone is only detectable from E15.5. (**A**) X-gal staining of whole-mount (left) or frozen sections of heart (right) of $GR^{+/-}$ foetuses demonstrates GR expression in heart at E10.5 (arrow, left), becoming widespread through the myocardium at E15.5. (**B**) Corticosterone content in C57BL/6J foetal heart increases after E14.5. Data analysed by one-way ANOVA with Bonferroni *post-hoc* test. $^{***}P < 0.001$ versus E14.5, $\#P < 0.05$ versus E15.5, $n = 6–16$. (**C**) Immunofluorescent co-staining of GR (red) with troponin T (green) in cardiomyocytes of $GR^{+/+}$ hearts from E10.5 shows negligible levels of GR within nuclei (DAPI) at or before E14.5 (merged images). Negative controls (E10.5 sections, omitting primary antibody) for immunofluorescent co-staining of GR with troponin T are shown as insets. Images representative of $n = 6$.

for GR in determination of placental blood flow and in renal function.

Heterozygous $GR^{+/-}$ mice showed an intermediate cardiac phenotype (Table 1). This predicts consequences for adult cardiovascular health in addition to the hypertension we previously described (12). A recent report of human GR haplo-insufficiency showed a strong association with hypertension similar to $GR^{+/-}$ mice (33), but other cardiovascular parameters were not examined. However, large population studies have linked a common haplotype of the GR gene associated with relative glucocorticoid resistance to increased risk of heart disease (34,35). The same GR polymorphism associates with systolic blood pressure and heart growth in early childhood (36) suggesting disease risk may be 'programmed" by prenatal glucocorticoid resistance. Moreover, in a family with an inactivating allele of the *NR3C1* gene encoding GR, premature coronary heart disease was associated with inheritance of the mutant *NR3C1* allele (37), suggesting association of heart disease with glucocorticoid resistance.

Although expressed in mouse heart from E10.5, GR is not activated until after E14.5, increasing to peak levels in little more than 24 h. This suggests that the heart may be exquisitely sensitive to perturbations in the normal developmental increase in glucocorticoids, with potential alterations in cardiac structure

Table 1. Comparison of the phenotypes of E17.5 $GR^{-/-}$, $GR^{+/-}$ and SMGRKO hearts

$GR^{-/-}$	$GR^{+/-}$	SMGRKO
GR protein levels in the heart		
None (non-functional chimeric protein)	50%	35% of levels in $GR^{fl/fl}$
Survival		
>50% die before birth	Present at 52% of foetuses at E17.5	No significant difference at E17.5
Oedema		
Excess fluid + increased body sodium	No excess fluid. Electrolytes not determined.	Similar phenotype, smaller magnitude
Heart size		
20% reduction in size	Not determined	No difference
Number of nuclei per field of view		
Increased	Not determined	Increased
Left ventricle compact myocardium–cardiomyocyte alignment		
Lacking a layer of rod-shaped aligned cells	Not determined	Similar phenotype
Myofibrils		
Short and disorganized	Not determined	Similar phenotype
Cardiac function (left ventricle)		
MPI increased, due to prolonged isovolumetric contraction and relaxation times	MPI increased, due to prolonged isovolumetric contraction and relaxation times	MPI increased, due to prolonged isovolumetric contraction time
E/A wave ratio decreased	No difference	No difference
Gene expression		
Decreased levels of mRNA encoding RyR2, SERCA2a, hexokinase-1	Decrease is not significant	Also decreased
Decreased levels of mRNA encoding ANP, MHCα	Also decreased	No difference

and function resulting from precocious or excessive glucocorticoid signalling. This is likely to be of clinical relevance. Synthetic glucocorticoids are routinely administered antenatally when preterm labour is threatened, well before the surge in endogenous foetal glucocorticoids that occurs close to term. GR is expressed in mid-gestation human heart (38). Thus, exogenous glucocorticoids may induce precocious cardiac maturation and a consequent inflexible phenotype.

Finally, our studies have other important clinical implications. $GR^{-/-}$ mice exhibit *hydrops fetalis*, a condition typified by widespread oedema in the foetus. Importantly, in SMGRKO the oedematous phenotype was also present, although of lower magnitude. In humans, *hydrops fetalis* is associated with a high mortality rate and occurs as the end-stage of a variety of disorders, particularly of cardiovascular origin. Glucocorticoids are an effective treatment in some cases (39) though it is unclear why. While we cannot directly attribute the oedema in GR-deficient mice to their cardiac defects, it nevertheless suggests that insufficient foetal glucocorticoid signalling could be a cause of *hydrops fetalis* in humans. This hypothesis deserves further investigation. Our data also have implications for the treatment of preterm infants. Serum cortisol levels are lower in these infants (40) who are at greater risk of sudden infant death syndrome than term babies. Heart immaturity may contribute to poor infant outcomes. Whether neonatal glucocorticoid treatment is beneficial in reducing later risk of sudden infant death syndrome merits investigation.

MATERIALS AND METHODS

Animals

$GR^{+/-}$ mice, heterozygous for a null mutation in the *Nr3c1* gene encoding GR (*Nr3c1*^{gtESK92MRCHGU} mice), have been previously described (12). $GR^{+/-}$ mice, congenic on the C57BL/6J background (>12 generations) were intercrossed to give $GR^{+/+}$, $GR^{+/-}$ and $GR^{-/-}$ foetal littermates. SMGRKO mice were generated by crossing SM22-Cre transgenic mice (16) with $GR^{fl/fl}$ mice (41) (obtained as frozen $GR^{fl/+}$ embryos from the European Mouse Mutant Archive; reference number 02124) and maintained by breeding $GR^{fl/fl}$ mice with SM22α-Cre^{+} $GR^{fl/fl}$ mice.

For measurement of heart corticosterone levels and RNA extraction, mice were time-mated between 1800–2200. The morning of the day the vaginal plug was found was designated E0.5. At specific time points, foetuses were collected. Genotyping was carried out on foetal tissue by PCR using *lacZ* primers for the *Nr3c1*^{gtESK92MRCHGU} allele (5′-GAGTTGCGTGACT ACCTACGG-3′ and 5′-GTACCACAGCGGATGGTTCGG-3′) and wild-type GR primers as described (12). In preliminary studies, the gender of foetuses was determined. Because no differences were observed between males and females (data not shown), data were pooled. SMGRKO mice were genotyped using primers for Cre recombinase (5′-GATCGCTGCCA GGATATACG-3′ and 5′- AGGCCAGGTATCTCTGACCA-3′).

For RNA extractions, western blotting and measurement of corticosterone content, foetal hearts were dissected and rapidly frozen on dry ice. For histopathology, foetuses were fixed in neutral buffered formalin, paraffin-embedded, sectioned (7 μm) and stained with haematoxylin and eosin (H&E). For other analyses, foetuses were processed as described in what follows. All animal experimentation was carried out in strict accord with accepted standards of humane animal care under the auspices of the Animal (Scientific Procedures) Act UK 1986 after prior approval by the University of Edinburgh Animal Ethical Review Committee.

Measurement of heart area

Total heart area was measured in H&E stained serial coronal sections of foetal heart using an MCID Basic 7.0 (InterFocus Imaging Ltd; Cambridge, UK) image analysis system, with the operator blind to genotype.

High-resolution ultrasound analysis

Analysis was performed *in vivo* on E17.5 foetuses using a Vevo 770 ultrasound biomicroscope (Visualsonics; Toronto, Canada). Pregnant mice were anaesthetized using isoflurane gas (initially 100% medical oxygen, then maintained at 1–2% isoflurane). Mice were laid supine with all legs taped to electrocardiogram electrodes to monitor the heart rate (around 450–550 bpm) and respiration of the pregnant dam. Body temperature was monitored using a rectal thermometer and was maintained at 36°C–38°C using a controlled heated table and infrared heat lamp. Abdominal hair was removed using a commercially available epilating cream and pre-warmed ultrasound gel (Aquasonic 100; Parker Laboratories, Orange, NJ, USA) was applied. The 30 MHz RMV 707B (real-time microvisualization) transducer was used, giving a focal length of 12.7 mm and a depth field view of 20 mm. The uterus was not exteriorized and 2–3 foetuses/dam were imaged transcutaneously over 20–30 min. Hearts were visualized in B-mode (standard pulse wave Doppler) (14,42,43). Transmitral Doppler traces were obtained from the longitudinal axis of the foetal hearts. Although individual foetal positions did not always allow an optimal Doppler angle to be achieved between the incident ultrasound beam and the direction of blood flow, variation in incident angle of the ultrasound with respect to the heart was no more than 5° between foetuses. No angle correction was made. Following imaging, the pregnant dam was euthanized *in situ*, scanned foetuses excised following identification by corroboration of position with the ultrasound images, then a tissue sample (tail or limb) taken from each foetus for genotyping.

High-throughput high-resolution micro-magnetic resonance imaging

MRI was carried out as described (44). E17.5 foetuses were immersion-fixed in 4% paraformaldehyde in phosphate-buffered saline (PBS) containing 2 mM dimeglumine gadopentetate (Gd-DTPA, Magnevist, Bayer Healthcare Pharmaceuticals, Wayne, NJ, USA) at 4°C. The heads were removed and the rest of the foetus was embedded in 1% agarose containing 2 mM Gd-DTPA in 28 mm multi-embryo imaging glass tubes (24/tube). Foetuses underwent μMRI scanning at a resolution of 25.4 × 25.4 × 24.4 μm per voxel. The volume data sets were visualized with the software package Amira 4.0 (Mercury Systems) and analysed using virtual re-sectioning. In selected foetuses, the heart, larger blood vessels and the trachea were manually reconstructed using the label field function of the software. Surface rendered 3D models were generated for presentation and to perform volume measurements. Ventricular volume was corrected for spine-sternum distance, which did not differ between genotypes.

Electron microscopy

Hearts were dissected from E17.5 foetuses and fixed in 3% glutaraldehyde in 0.1 M sodium cacodylate, pH 7.3, post-fixed in 1% osmium tetroxide in 0.1 M sodium cacodylate, then dehydrated and embedded in araldite resin. Ultrathin (60 nm) sections were cut and stained in uranyl acetate and lead citrate then viewed in a Phillips CM120 Transmission electron microscope (FEI UK Ltd, Cambridge, UK).

Western blotting

Myosin heavy chain α (MyHCα) levels were measured by western blot using 1:200 dilution mouse anti-cardiac myosin heavy chain primary antibody (Abcam, Cambridge, UK) with fluorophore-conjugated secondary antibodies (Alexa Fluor, Invitrogen, Paisley, UK). Protein levels were measured relative to β-tubulin levels using an Odyssey infrared imaging system (Licor Biosciences, Lincoln, NE, USA).

Immunohistochemistry

Sections were dewaxed, hydrated, boiled in 0.1 M citric acid buffer and blocked using standard protocols before overnight incubation with anti-troponin T antibody (Abcam, Cambridge, UK), M20 rabbit polyclonal anti-GR antibody (Santa Cruz Biotechnology, Santa Cruz, CA, USA) or FITC-wheat germ agglutinin (FITC-WGA, Invitrogen) according to manufacturer's protocols. Fluorophore-conjugated secondary antibodies (Alexa Fluor, Invitrogen;) or biotinylated secondary antibody with Vectastain Elite ABC reagent (Vector Labs, Peterborough, UK) were used to detect immunostaining.

X-gal staining

X-gal (5-bromo-4-chloro-3-indolyl-beta-D-galacto-pyranoside) staining to detect β-galactosidase activity was performed as described (12) on whole embryos or dissected heart and lung, fixed in 0.2% glutaraldehyde or frozen sections post-fixed in 4% paraformaldehyde. Briefly, tissues were stained overnight at 37°C in PBS containing 2 mM $MgCl_2$, 0.02% NP-40, 0.01% sodium deoxycholate, 5 mM potassium ferricyanide, 5 mM potassium ferrocyanide, 1 mg/ml X-gal. Some X-gal-stained embryos were visualized by OPT microscopy (45). Briefly, embryos were mounted in 1% agarose, dehydrated in methanol, cleared in benzyl alcohol:benzyl benzoate (1:2 v/v) and imaged using a Bioptonics 3001 OPT scanner (Bioptonics, Edinburgh, UK) with brightfield to detect X-gal staining and tissue autofluorescence (excitation 425 nm/emission 475 nm) to capture the anatomy. The resulting images were reconstructed, automatically thresholded and merged to a single 3D image using NRecon software (Skyscan, Belgium) and Bioptonics Viewer (Bioptonics, Edinburgh, UK).

Dessication and whole-body electrolyte measurement

E17.5 and E18.5 foetuses were weighed immediately after dissection, placed in an open-lid plastic container and incubated in an oven at 60°C for 5 days. Dry weight was recorded. Whole embryo sodium and potassium contents were measured by flame photometry as described (46) and corrected for body weight.

Measurement of heart corticosterone content

Steroids were extracted from C57BL/6J foetal hearts following homogenization in ice-cold 5 mM potassium phosphate buffer.

The homogenate was dripped slowly into pre-chilled ethanol (95%) containing glacial acetic acid (3% v/v), stored overnight at −80°C then sonicated (1–2 min) in a chilled container. Following centrifugation, the supernatant was evaporated to dryness under N_2 at 60°C, dissolved in methanol (0.5 ml, 80% v/v), then 0.5 ml H_2O added and applied to an activated C18 Sep-pak column (Waters Corporation, Milford, MA, USA). After washing with H_2O and methanol (40% v/v), steroids were eluted in 2 ml methanol. The solvent was evaporated as earlier and steroids reconstituted in borate buffer (0.13 M H_3BO_3, 0.067 M NaOH, pH 7.4) containing 0.5% BSA, 1% methanol and 0.1% ethylene glycol. Corticosterone was measured using a competitive radioimmunoassay as previously described (12) and expressed relative to protein content.

Quantitative (q)PCR

RNA was extracted using an RNAeasy kit (Qiagen) according to the manufacturer's instructions and reverse transcribed using a Superscript First Strand Synthesis kit (Invitrogen Ltd, Paisley, UK). Quantitative (q)PCR was carried out using a LightCycler 480 (Roche Diagnostics Ltd, Burgess Hill, UK) with a commercial master mix (LC 480 Probes Master) and either Taqman primer/probe sets (Ambion; Austin, TX, USA) or using the Universal Probe Library system (Roche Diagnostics Ltd, Burgess Hill, UK) (Supplementary Material, Table S1). Data were analysed using the second derivative maximum method. The ratio of the levels of the transcript of interest to the levels of TATA Binding Protein mRNA (internal control) was determined for each sample.

Statistics

All numerical data are presented as mean ± SEM. Statistical evaluation was carried out with Prism (GraphPad) and used Student's *t*-test, Mann–Whitney U-test, one-way ANOVA with Bonferroni *post-hoc* test or two-way ANOVA with Bonferroni multiple comparisons *post-hoc* test, as appropriate.

SUPPLEMENTARY MATERIAL

Supplementary Material is available at *HMG* online.

ACKNOWLEDGEMENTS

We thank Wiktoria Wyrzykowska, Isla Thomson, Emma Charlton and Nur Saffie for assistance with histology and quantification of histology, staff at the University of Edinburgh Biomedical Research Resources facility for assistance with animal care and Steve Mitchell for transmission electron microscopy. We are grateful to Jonathan Bard, Matt Kaufman, Sebastian Pieperhoff, Emma Di Rollo, Caitlin Wyrwoll, Marianne Keith and Chris Gregory for expert advice and/or assistance and thank Martin Denvir, Gillian Gray and Jonathan Seckl for their helpful comments on the manuscript.

Conflict of Interest statement. None declared.

FUNDING

This work was supported by a British Heart Foundation PhD studentship (to E.R.-Z.).

REFERENCES

1. Fowden, A.L., Li, J. and Forhead, A.J. (1998) Glucocorticoids and the preparation for life after birth: are there long-term consequences of the life insurance? *Proc. Nutr. Soc.*, **57**, 113–122.
2. Michelsohn, A.M. and Anderson, D.J. (1992) Changes in competence determine the timing of 2 sequential glucocorticoid effects on sympathoadrenal progenitors. *Neuron*, **8**, 589–604.
3. Seckl, J.R. and Holmes, M.C. (2007) Mechanisms of disease: glucocorticoids, their placental metabolism and fetal 'programming' of adult pathophysiology. *Nat. Clin. Pract. Endocrinol. Metab.*, **3**, 479–488.
4. Miracle, X., Di Renzo, G.C., Stark, A., Fanaroff, A., Carbonell-Estrany, X. and Saling, E. (2008) Guideline for the use of antenatal corticosteroids for fetal maturation. *J. Perinat. Med.*, **36**, 191–196.
5. Cole, T., Blendy, J.A., Monaghan, A.P., Kriegelstein, K., Schmid, W., Fantuzzi, G., Hummler, E., Unsicker, K. and Schütz, G. (1995) Targeted disruption of the glucocorticoid receptor blocks adrenergic chromaffin cell development and severely retards lung maturation. *Genes. Dev.*, **9**, 1608–1621.
6. Opherk, C., Tronche, F., Kellendonk, C., Kohlmuller, D., Schulze, A., Schmid, W. and Schutz, G. (2004) Inactivation of the glucocorticoid receptor in hepatocytes leads to fasting hypoglycemia and ameliorates hyperglycemia in streptozotocin-induced diabetes mellitus. *Mol. Endocrinol.*, **18**, 1346–1353.
7. Tangalakis, K., Lumbers, E.R., Moritz, K.M., Towstoless, M.K. and Wintour, E.M. (1992) Effect of cortisol on blood pressure and vascular reactivity in the ovine fetus. *Exp. Physiol.*, **77**, 709–717.
8. Mulder, E.J., de Heus, R. and Visser, G.H. (2009) Antenatal corticosteroid therapy: short-term effects on fetal behaviour and haemodynamics. *Semin. Fetal Neonatal. Med.*, **14**, 151–156.
9. Torres, A., Belser, W.W. III, Umeda, P.K. and Tucker, D. (1997) Indicators of delayed maturation of rat heart treated prenatally with dexamethasone. *Pediatr. Res.*, **42**, 139–144.
10. Giraud, G.D., Louey, S., Jonker, S., Schultz, J. and Thornburg, K.L. (2006) Cortisol stimulates cell cycle activity in the cardiomyocyte of the sheep fetus. *Endocrinology*, **147**, 3643–3649.
11. Slotkin, T.A., Seidler, F.J., Kavlock, R.J. and Bartolome, J.V. (1991) Fetal dexamethasone exposure impairs cellular development in neonatal rat heart and kidney: effects on DNA and protein in whole tissues. *Teratology*, **43**, 301–306.
12. Michailidou, Z., Carter, R.N., Marshall, E., Sutherland, H.G., Brownstein, D.G., Owen, E., Cockett, K., Kelly, V., Ramage, L., Al-Dujaili, E.A. *et al.* (2008) Glucocorticoid receptor haploinsufficiency causes hypertension and attenuates hypothalamic-pituitary-adrenal axis and blood pressure adaptions to high-fat diet. *FASEB J.*, **22**, 3896–3907.
13. Nemati, B., Atmodjo, W., Gagnon, S., Humes, D., McKerlie, C., Kaplan, F. and Sweezey, N.B. (2008) Glucocorticoid receptor disruption delays structural maturation in the lungs of newborn mice. *Pediatr. Pulmonol.*, **43**, 125–133.
14. Tei, C., Ling, L.H., Hodge, D.O., Bailey, K.R., Oh, J.K., Rodeheffer, R.J., Tajik, A.J. and Seward, J.B. (1995) New index of combined systolic and diastolic myocardial performance: a simple and reproducible measure of cardiac function–a study in normals and dilated cardiomyopathy. *J. Cardiol.*, **26**, 357–366.
15. Zhou, Y.Q., Foster, F.S., Parkes, R. and Adamson, S.L. (2003) Developmental changes in left and right ventricular diastolic filling patterns in mice. *Am. J. Physiol. Heart Circ. Physiol.*, **285**, H1563–1575.
16. Boucher, P., Gotthardt, M., Li, W.P., Anderson, R.G. and Herz, J. (2003) LRP: role in vascular wall integrity and protection from atherosclerosis. *Science*, **300**, 329–332.
17. Li, L., Miano, J.M., Cserjesi, P. and Olson, E.N. (1996) SM22 alpha, a marker of adult smooth muscle, is expressed in multiple myogenic lineages during embryogenesis. *Circ. Res.*, **78**, 188–195.
18. Langlois, D., Hneino, M., Bouazza, L., Parlakian, A., Sasaki, T., Bricca, G. and Li, J.Y. (2010) Conditional inactivation of TGF-beta type II receptor in smooth muscle cells and epicardium causes lethal aortic and cardiac defects. *Transgenic Res.*, **19**, 1069–1082.

19. Malhowski, A.J., Hira, H., Bashiruddin, S., Warburton, R., Goto, J., Robert, B., Kwiatkowski, D.J. and Finlay, G.A. (2011) Smooth muscle protein-22-mediated deletion of Tsc1 results in cardiac hypertrophy that is mTORC1-mediated and reversed by rapamycin. *Hum. Mol. Genet.*, **20**, 1290–1305.
20. Wang, J.C., Derynck, M.K., Nonaka, D.F., Khodabakhsh, D.B., Haqq, C. and Yamamoto, K.R. (2004) Chromatin immunoprecipitation (ChIP) scanning identifies primary glucocorticoid receptor target genes. *Proc. Natl Acad. Sci. USA*, **101**, 15603–15608.
21. Sai, S., Esteves, C.L., Kelly, V., Michailidou, Z., Anderson, K., Coll, A.P., Nakagawa, Y., Ohzeki, T., Seckl, J.R. and Chapman, K.E. (2008) Glucocorticoid regulation of the promoter of 11β-hydroxysteroid dehydrogenase type 1 is indirect and requires C/EBPβ. *Mol. Endocrinol.*, **22**, 2049–2060.
22. Muzikar, K.A., Nickols, N.G. and Dervan, P.B. (2009) Repression of DNA-binding dependent glucocorticoid receptor-mediated gene expression. *Proc. Natl Acad. Sci. USA,* **106**, 16598–16603.
23. Buckberg, G., Hoffman, J.I., Mahajan, A., Saleh, S. and Coghlan, C. (2008) Cardiac mechanics revisited: the relationship of cardiac architecture to ventricular function. *Circulation*, **118**, 2571–2587.
24. Jones, W.K., Grupp, I.L., Doetschman, T., Grupp, G., Osinska, H., Hewett, T.E., Boivin, G., Gulick, J., Ng, W.A. and Robbins, J. (1996) Ablation of the murine alpha myosin heavy chain gene leads to dosage effects and functional deficits in the heart. *J. Clin. Invest.*, **98**, 1906–1917.
25. Herron, T.J. and McDonald, K.S. (2002) Small amounts of alpha-myosin heavy chain isoform expression significantly increase power output of rat cardiac myocyte fragments. *Circ. Res.*, **90**, 1150–1152.
26. Miyata, S., Minobe, W., Bristow, M.R. and Leinwand, L.A. (2000) Myosin heavy chain isoform expression in the failing and nonfailing human heart. *Circ. Res.*, **86**, 386–390.
27. Bellini, C., Hennekam, R.C., Fulcheri, E., Rutigliani, M., Morcaldi, G., Boccardo, F. and Bonioli, E. (2009) Etiology of nonimmune hydrops fetalis: a systematic review. *Am. J. Med. Genet. A.*, **149A**, 844–851.
28. Schulz-Baldes, A., Berger, S., Grahammer, F., Warth, R., Goldschmidt, I., Peters, J., Schutz, G., Greger, R. and Bleich, M. (2001) Induction of the epithelial Na+ channel via glucocorticoids in mineralocorticoid receptor knockout mice. *Pflugers Arch.*, **443**, 297–305.
29. Nguyen Dinh Cat, A., Ouvrard-Pascaud, A., Tronche, F., Clemessy, M., Gonzalez-Nunez, D., Farman, N. and Jaisser, F. (2009) Conditional transgenic mice for studying the role of the glucocorticoid receptor in the renal collecting duct. *Endocrinology*, **150**, 2202–2210.
30. Bailey, M.A., Mullins, J.J. and Kenyon, C.J. (2009) Mineralocorticoid and glucocorticoid receptors stimulate epithelial sodium channel activity in a mouse model of Cushing syndrome. *Hypertension*, **54**, 890–896.
31. Cameron, V.A. and Ellmers, L.J. (2003) Minireview: natriuretic peptides during development of the fetal heart and circulation. *Endocrinology*, **144**, 2191–2194.
32. Scott, N.J., Ellmers, L.J., Lainchbury, J.G., Maeda, N., Smithies, O., Richards, A.M. and Cameron, V.A. (2009) Influence of natriuretic peptide receptor-1 on survival and cardiac hypertrophy during development. *Biochim. Biophys. Acta.*, **1792**, 1175–1184.
33. Bouligand, J., Delemer, B., Hecart, A.-C., Meduri, G., Viengchareun, S., Amazit, L., Trabado, S., Feve, B., Guiochon-Mantel, A., Young, J. *et al.* (2010) Familial glucocorticoid receptor haploinsufficiency by non-sense mediated mRNA decay, adrenal hyperplasia and apparent mineralocorticoid excess. *PLoS ONE*, **5**, e13563.
34. van den Akker, E.L., Koper, J.W., van Rossum, E.F., Dekker, M.J., Russcher, H., de Jong, F.H., Uitterlinden, A.G., Hofman, A., Pols, H.A., Witteman, J.C. *et al.* (2008) Glucocorticoid receptor gene and risk of cardiovascular disease. *Arch. Intern. Med.*, **168**, 33–39.
35. Otte, C., Wust, S., Zhao, S., Pawlikowska, L., Kwok, P.-Y. and Whooley, M.A. (2010) Glucocorticoid receptor gene, low-grade inflammation, and heart failure: the heart and soul study. *J. Clin. Endocrinol. Metab.*, **95**, 2885–2891.
36. Geelhoed, J.J., van Duijn, C., van Osch-Gevers, L., Steegers, E.A., Hofman, A., Helbing, W.A. and Jaddoe, V.W. (2011) Glucocorticoid receptor-9beta polymorphism is associated with systolic blood pressure and heart growth during early childhood. The Generation R Study. *Early Hum. Dev.*, **87**, 97–102.
37. Donner, K.M., Hiltunen, T.P., Janne, O., Sane, T. and Kontula, K. (2012) Generalized glucocorticoid resistance caused by a novel two nucleotide deletion in the hormone binding domain of the glucocorticoid receptor gene NR3C1. *Eur. J. Endocrinol.*, **168**, K9–K18.
38. Ballard, P.L. and Ballard, R.A. (1974) Cytoplasmic receptor for glucocorticoids in lung of the human fetus and neonate. *J. Clin. Invest.*, **53**, 477–486.
39. Tsao, K., Hawgood, S., Vu, L., Hirose, S., Sydorak, R., Albanese, C.T., Farmer, D.L., Harrison, M.R. and Lee, H. (2003) Resolution of hydrops fetalis in congenital cystic adenomatoid malformation after prenatal steroid therapy. *J. Pediatr. Surg.*, **38**, 508–510.
40. Naeye, R.L., Harcke, H.T. Jr. and Blanc, W.A. (1971) Adrenal gland structure and the development of hyaline membrane disease. *Pediatrics*, **47**, 650–657.
41. Tronche, F., Kellendonk, C., Kretz, O., Gass, P., Anlag, K., Orban, P.C., Bock, R., Klein, R. and Schutz, G. (1999) Disruption of the glucocorticoid receptor gene in the nervous system results in reduced anxiety. *Nat. Genet.*, **23**, 99–103.
42. Shen, Y., Leatherbury, L., Rosenthal, J., Yu, Q., Pappas, M.A., Wessels, A., Lucas, J., Siegfried, B., Chatterjee, B., Svenson, K. *et al.* (2005) Cardiovascular phenotyping of fetal mice by noninvasive high-frequency ultrasound facilitates recovery of ENU-induced mutations causing congenital cardiac and extracardiac defects. *Physiol. Genomics*, **24**, 23–36.
43. Corrigan, N., Brazil, D.P. and McAuliffe, F.M. (2010) High-frequency ultrasound assessment of the murine heart from embryo through to juvenile. *Reprod. Sci.*, **17**, 147–157.
44. Schneider, J.E., Bose, J., Bamforth, S.D., Gruber, A.D., Broadbent, C., Clarke, K., Neubauer, S., Lengeling, A. and Bhattacharya, S. (2004) Identification of cardiac malformations in mice lacking Ptdsr using a novel high-throughput magnetic resonance imaging technique. *BMC Dev. Biol.*, **4**, 16.
45. Sharpe, J., Ahlgren, U., Perry, P., Hill, B., Ross, A., Hecksher-Sorensen, J., Baldock, R. and Davidson, D. (2002) Optical projection tomography as a tool for 3D microscopy and gene expression studies. *Science*, **296**, 541–545.
46. Kenyon, C.J., Brown, W.B., Fraser, R., Tonolo, G., McPherson, F. and Davies, D.L. (1990) Effects of dexamethasone on body fluid and electrolyte composition of rats. *Acta Endocrinol. (Copenh.)*, **122**, 599–604.